Journal of Power Sources 234 (2013) 23–30

Contents lists available at SciVerse ScienceDirect

Journal of Power Sources

journal homepage: www.elsevier.com/locate/jpowsour

A new class of organic dyes containing β-substituted 2, 2′-bithiophenene unit as a π-linker for dye-sensitized solar cells: Structural modification for understanding relationship of structure and photovoltaic performances

Tainan Duan [1], Ke Fan [1], Cheng Zhong [1], Xingguo Chen*, Tianyou Peng*, Jingui Qin [1]

Hubei Key Laboratory on Organic and Polymeric Opto-electronic Materials, College of Chemistry and Molecular Sciences, Wuhan University, Wuhan 430072, China

HIGHLIGHTS

- New D-π-A organic dyes containing a π-linker of 2,2′-bithiophene unit have been obtained.
- The dye with good coplanar structure exhibits excellent photovoltaic performances.
- The structure–performance relationship is explored with the aid of theoretical calculation.

GRAPHICAL ABSTRACT

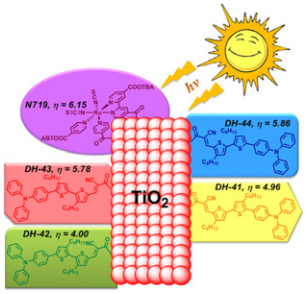

ARTICLE INFO

Article history:
Received 7 October 2012
Received in revised form
26 December 2012
Accepted 19 January 2013
Available online 29 January 2013

Keywords:
Organic dyes
Dye-sensitized solar cells
Photovoltaic performances
D-π-A structure

ABSTRACT

A new class of metal-free organic dyes (**DH-41**–**DH-44**) containing triphenylamine group as an electron donor, cyanoacrylic acid group as an electron acceptor and a π-linker of 2,2′-bithiophene unit with two hexyl groups at different β-substituted positions have been designed and synthesized. Their photovoltaic performances are characterized experimentally and the structure–performance relationship is explored with the aid of theoretical calculation. Although all the DH dyes show the same structural backbone, changing β-substituted positions of hexyl group at 2,2′-bithiophene unit can alter the molecular coplanarity of conjugated skeleton and the intramolecular charge transfer (ICT) that finally affects the UV–Vis absorption and the photovoltaic performances of the DH dyes. By comparison, the dyes with two hexyl groups at nonortho β-positions of 2,2′-bithiophene unit shows less steric hindrance and better molecular coplanarity that is favorable for improving photovoltaic performances. Among them, **DH-44** has the best optimized structure for ICT, so it shows broadened and red-shifted absorption with high molar extinction coefficient, and exhibits excellent photovoltaic performances with high power conversion efficiency of 5.86%, which reaches over 95% of the reference dye N719-based cell fabricated and measured under the same conditions.

1. Introduction

Since the first report by O'Regan and Grätzel in 1991, [1] dye-sensitized solar cells (DSSCs) has aroused ever-increasing interest in both scientists and engineers due to the high power conversion efficiency and low production cost that endows it as a powerful competitor to conventional silicon-based photovoltaic devices. [2] The sensitizers as the most crucial element in DSSCs have been attracted considerable attention, and a large number of new sensitizers have been designed and synthesized [3–7]. Compared with traditional ruthenium complex dyes, metal-free organic dyes have become more promising for DSSCs since they exhibit the high

* Corresponding authors. Tel.: +86 27 68755655; fax: +86 27 68756757.
E-mail addresses: xgchen@whu.edu.cn (X. Chen), typeng@whu.edu.cn (T. Peng).
[1] Tel.: +86 27 68755655; fax: +86 27 68756757.

0378-7753/$ – see front matter © 2013 Elsevier B.V. All rights reserved.
http://dx.doi.org/10.1016/j.jpowsour.2013.01.127

molar extinction coefficient, low-cost device fabrication, and easily molecular modification and tailoring [8]. Therefore, in the past decade various functional groups have been arranged and combined to generate D-π-A structural organic sensitizers for DSSCs. Among them, triphenylamine (TPA), thiophene derivative and cyanoacrylic acid moieties are the most commonly employed subunits for the electron donor, π-linker and electron acceptor/anchoring group, respectively [9–13]. For example, Daeneke et al. recently designed and synthesized a D-π-A sensitizer (Carbz-PAHTDTT) with this classic combination that exhibited much high efficiency with non-classic ferrocene-based electrolytes [14].

As a conjugated bridge that connects the donor and acceptor, π-linker exerts a significant influence on the charge transmission and recombination during the photo-electric conversion process in DSSCs [15–17], which leads to much difference for the photovoltaic performances as well as the device stability. Oligothiophene, especially β-substituted alkyl oligothiophene, is a popular choice for π-linker due to its electron-rich property, good thermal and electrochemical stability. In addition, β-substituted alkyl chain can suppress the charge recombination and enhance the open-circuit voltage effectively [18]. Thus, introducing oligothiophene unit as π-linker into the skeleton of sensitizer and changing β-substituted position of alkyl chain at thiophene ring have been explored to constitute various configurations for DSSCs [19–23].

In order to further understand the correlation of structure and photovoltaic performances via modifying π-linker to design new sensitizers and optimize the performance of DSSCs, we choose 2,2′-bithiophene unit, a classic linker as a template, to construct D-π-A sensitizers. By changing β-substituted positions of n-hexyl group at 2,2′-bithiophene unit, a series of dyes (**DH-41**–**DH-44** as shown in Fig. 1) containing triphenylamine (TPA) group as an electron-donor and cyanoacrylic acid group as an electron acceptor/anchoring group have been synthesized. The photophysical properties, electrochemical properties have been studied, and the photovoltaic performances as well as the structure–performance relationship have also been explored by experiments and elucidated with the aid of theoretical calculation.

2. Experimental

2.1. Equipments and materials

^{1}H NMR and ^{13}C NMR spectra were measured with a Varian MERCURY-VX300 in $CDCl_3$ or in d_6-DMSO with TMS as internal reference. UV–Vis absorption spectrometry was performed on a Shimadzu UV-3600 spectrophotometer. The electrochemical behaviors were investigated by using cyclic voltammetry (CV) on a CHI600A electrochemical work station. The elemental analysis was carried out on a CARLOERBA-1106 microelemental analyzer. Mass spectra were recorded with a VJ-ZAB-3F-Mass spectrometer or a Bruker 320-MS triple quadrupole mass spectrometer.

The catalyst of $Pd(PPh_3)_4$ was synthesized in our own lab, and anhydrous solvents used in Schlenk system was purified by refluxing with Na–K alloy. Some other reagents and solvents were commercially purchased and used without further purification. Compound **1**, [24] **2**, [25] **3**, [26] **4**, [27] and **5** [28] were prepared according to the corresponding literature.

2.2. Synthesis

2.2.1. 3′,4-Dihexyl-2,2′-bithiophene-5-carbaldehyde (**6**)

5′-Bromo-3,4′-dihexyl-2,2′-bithiophene (**5**) (2.11 g, 5.1 mmol) was dissolved in 60 mL anhydrous THF in a well-dried flask under the protection of argon atmosphere. N-Butyl lithium (2.3 mL, 5.5 mmol, 2.4 M in hexane) was added dropwise by syringe at −78 °C. After the addition, the reaction mixture was stirred at −78 °C for 1 h and anhydrous DMF (0.5 mL, 6.6 mmol) was added dropwise, then the mixture was warmed to room temperature. After stirring overnight, the mixture was quenched with water and extracted with ethyl acetate. The organic layer was washed with brine and dried over anhydrous Na_2SO_4. After removing the solvent, the residue was purified by column chromatography on silica gel (petroleum ether/CH_2Cl_2, 3:1) to give compound **6** as pale brown oil (1.31 g, 3.6 mmol, 71%). ^{1}H NMR (300 MHz, $CDCl_3$, δ ppm): 10.01 (s, 1H), 7.26 (d, 1H, J = 5.1 Hz), 7.03 (s, 1H), 6.97 (d, 1H, J = 5.1 Hz), 2.97 (t, 2H, J = 7.5 Hz), 2.84 (t, 2H, J = 8.1 Hz), 1.72–1.95 (m, 4H), 1.38–1.32 (m, 12H), 0.89–0.88 (m, 6H). ^{13}C NMR (75 MHz, $CDCl_3$, δ ppm): 181.9, 153.5, 145.7, 142.1, 136.5, 130.8, 130.0, 128.6, 125.6, 31.8, 31.7, 31.5, 30.5, 29.7, 29.4, 29.1, 28.6, 22.8, 14.2. MS (EI): m/Z = 362.

2.2.2. 5′-Bromo-3′,4-dihexyl-2,2′-bithiophene-5-carbaldehyde (**7**)

To a 3′,4-dihexyl-2,2′-bithiophene-5-carbaldehyde (**6**) (1.09 g, 3.0 mmol) in DMF (15 mL), a solution of N-bromosuccinimide (534 mg, 3 mmol) in DMF (8 mL) was added dropwise. After stirring overnight at room temperature in darkness, the resulting solution was poured into ice water (100 mL) and extracted with dichloromethane (50 mL × 2). The organic phase was washed with water and brine, dried over anhydrous Na_2SO_4, and filtered. The solvent was removed and the residue was purified by column chromatography on silica gel (petroleum ether/CH_2Cl_2, 3:1) to obtain the target compound (**7**) as yellow oil (1.22 g (2.77 mmol, 92%). ^{1}H NMR (300 MHz, $CDCl_3$, δ ppm): 10.00 (s, 1H), 6.95 (s, 1H), 6.92 (s, 1H),

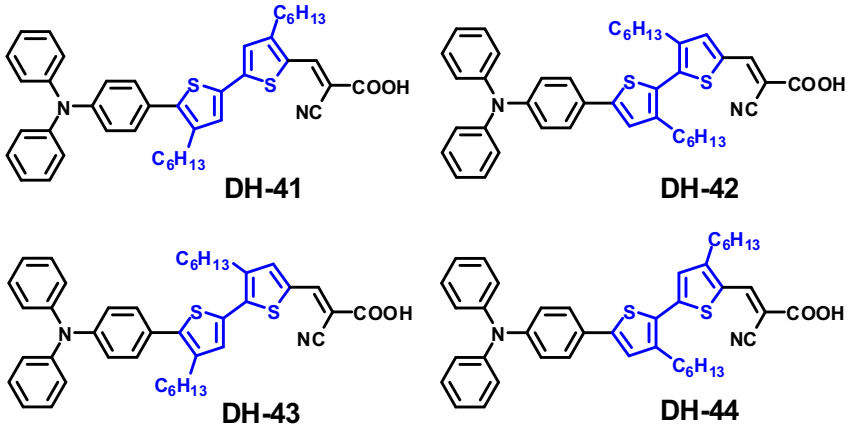

Fig. 1. Molecular structure of DH dyes.

2.93 (t, 2H, J = 7.5 Hz), 2.74 (t, 2H, J = 7.8 Hz), 1.69–1.61 (m, 4H), 1.33–1.23 (m, 12H), 0.89–0.85 (m, 6H). ^{13}C NMR (75 MHz, $CDCl_3$, δ ppm): 181.7, 153.3, 143.9, 142.5, 136.8, 131.4, 129.1, 128.7, 127.3, 31.7, 31.5, 30.8, 30.3, 29.6, 29.2, 29.1, 28.5, 22.7, 14.2. MS (EI): m/Z = 441.

*2.2.3. Aldehyde **8**–**11***

In a Schlenk tube, N,N-diphenyl-4-(4,4,5,5-tetramethyl-1,3,2-dioxaborolan-2-yl)aniline (**1**) (1.1 equiv.), aldehyde (**2**–**4,7**) (1 equiv.), $Pd(PPh_3)_4$ (0.04 equiv.) and K_2CO_3 (8 equiv.) were dissolved in a degassed mixed solvent of THF/H_2O. The mixture was heated at 65 °C under an argon atmosphere for 2 days. After reaction, the organic phase was separated, dried over anhydrous Na_2SO_4 and filtered. The filtrate was evaporated to dryness and purified by silica gel column chromatography with petroleum ether/CH_2Cl_2 (1:1) as eluent to afford target aldehyde (**8**–**11**).

*2.2.3.1. 5′-(4-(Diphenylamino)phenyl)-4,4′-dihexyl-2,2′-bithiophene-5-carbaldehyde (**8**).* Orange Oil, Yield: 80%. ^{1}H NMR (300 MHz, $CDCl_3$, δ ppm): 9.95 (s, 1H), 7.27–7.22 (m, 6H), 7.19 (s, 1H), 7.13–7.10 (m, 4H), 7.08 (s, 1H), 7.05–7.01 (m, 4H), 2.88 (t, 2H), 2.63 (t, 2H), 1.70–1.59 (m, 4H), 1.32–1.24 (m, 12H), 0.89–0.85 (m, 6H). ^{13}C NMR (75 MHz, $CDCl_3$, δ ppm): 181.2, 153.8, 147.5, 147.3, 146.3, 139.8, 139.5, 135.3, 133.3, 129.7, 129.4, 128.6, 127.2, 125.9, 124.8, 123.4, 122.7, 31.6, 31.4, 30.9, 29.2, 29.0, 28.8, 28.5, 22.6, 21.0, 14.1. MS (ESI): m/Z = 605.3.

*2.2.3.2. 5′-(4-(Diphenylamino)phenyl)-3,3′-dihexyl-2,2′-bithiophene-5-carbaldehyde (**9**).* Orange Oil, Yield: 77%. ^{1}H NMR (300 MHz, $CDCl_3$, δ ppm): 9.86 (s, 1H), 7.65 (s, 1H), 7.47 (d, 2H), 7.30–7.26 (m, 4H), 7.14–7.03 (m, 9H), 2.64 (t, 2H), 2.56 (t, 2H), 1.58 (br, 4H), 1.26 (br, 12H), 0.86–0.84 (m, 6H). ^{13}C NMR (75 MHz, $CDCl_3$, δ ppm): 182.9, 147.7, 147.4, 144.9, 144.3, 143.6, 142.4, 140.2, 137.9, 129.4, 127.7, 126.6, 125.7, 124.7, 124.2, 123.6, 123.3, 31.7, 30.8, 30.6, 29.3, 29.2, 29.1, 29.0, 28.9, 22.7, 14.1. MS (ESI): m/Z = 606.9.

*2.2.3.3. 5′-(4-(Diphenylamino)phenyl)-3,4′-dihexyl-2,2′-bithiophene-5-carbaldehyde (**10**).* Orange Oil, Yield: 89%. ^{1}H NMR (300 MHz, $CDCl_3$, δ ppm): 9.81 (s, 1H), 7.58 (s, 1H), 7.32–7.26 (m, 6H), 7.16–7.04 (m, 9H), 2.85 (t, 2H), 2.69 (t, 2H), 1.69–1.61 (m, 4H), 1.30–1.26 (m, 12H), 0.89–0.88 (m, 6H). ^{13}C NMR (75 MHz, $CDCl_3$, δ ppm): 182.5, 147.6, 147.5, 142.0, 140.4, 139.9, 139.3, 139.1, 132.4, 130.1, 129.9, 129.5, 127.4, 124.9, 123.5, 122.9, 122.7, 31.8, 31.0, 30.4, 29.8, 29.6, 29.3, 28.9, 25.5, 22.8, 14.3. MS (ESI): m/Z = 606.7.

*2.2.3.4. 5′-(4-(Diphenylamino)phenyl)-3′,4-dihexyl-2,2′-bithiophene-5-carbaldehyde (**11**).* Orange Oil, Yield: 85%. ^{1}H NMR (300 MHz, $CDCl_3$, δ ppm): 10.00 (s, 1H), 7.46 (d, 2H), 7.31–7.26 (m, 4H), 7.14 (d, 4H), 7.08–7.04 (m, 6H), 2.96 (t, 2H), 2.84 (t, 2H), 1.71–1.69 (m, 4H), 1.42–1.26 (m, 12H), 0.89 (br, 6H). ^{13}C NMR (75 MHz, $CDCl_3$, δ ppm): 181.0, 152.9, 147.5, 147.0, 145.2, 143.5, 142.9, 135.6, 129.1, 128.1, 127.4, 126.9, 126.1, 125.4, 124.0, 123.1, 122.9, 31.4, 31.3, 31.1, 29.8, 29.1, 28.8, 28.1, 24.6, 22.4, 13.9. MS (ESI): m/Z = 606.3.

*2.2.4. **DH** dyes (**DH-41**–**DH-44**)*

A mixture of the aldehyde (**8**–**11**) (1.0 equiv.), cyanoacetic acid (10.0 equiv.), and ammonium acetate (0.5 equiv.) were placed in a flask in acetic acid under an argon atmosphere with heating 130 °C for 12 h. After cooling, the reaction was quenched by adding water, and extracted with dichloromethane (DCM). The organic layer was dried over anhydrous Na_2SO_4. After removing the solvent, the crude product was purified by silica gel column chromatograph eluted with toluene/methanol (10/1), the target dyes was isolated as a powder.

*2.2.4.1. (E)-2-Cyano-3-(5′-(4-(diphenylamino)phenyl)-4,4′-dihexyl-2,2′-bithiophene-5-yl)acrylic acid (**DH-41**).* Crimson powder. Yield: 69%. ^{1}H NMR (300 MHz, d_6-DMSO, δ ppm): 8.28 (s, 1H), 7.52 (s, 1H), 7.46 (s, 1H), 7.37–7.32 (m, 6H), 7.13–7.06 (m, 5H), 7.00–6.97 (m, 3H), 2.80 (t, 2H), 2.65 (t, 2H), 1.59 (br, 4H), 1.28–1.23 (m, 12H), 0.85–0.82 (m, 6H). ^{13}C NMR (75 MHz, $CDCl_3$, δ ppm): 169.3, 157.7, 148.1, 147.9, 147.5, 145.0, 141.3, 140.2, 132.9, 129.9, 129.6, 128.8, 127.2, 125.6, 125.1, 123.7, 123.0, 122.7, 116.5, 94.0, 31.8, 31.4, 31.1, 30.6, 29.4, 29.2, 22.8, 21.0, 14.3. MS (ESI): m/Z = 672.9. $C_{42}H_{44}N_2O_2S_2$ (M_w = 672.94): calcd. C, 74.96; H, 6.59; N, 4.16; found C, 74.85; H, 6.83; N, 4.22.

*2.2.4.2. (E)-2-Cyano-3-(5′-(4-(diphenylamino)phenyl)-3,3′-dihexyl-2,2′-bithiophene-5-yl)acrylic acid (**DH-42**).* Red powder. Yield: 68%. ^{1}H NMR (300 MHz, d_6-DMSO, δ ppm): 8.46 (s, 1H), 7.97 (s, 1H), 7.60–7.54 (m, 3H), 7.44 (s, 1H), 7.36–7.30 (m, 5H), 7.10–7.04 (m, 6H), 2.89 (t, 2H), 2.82 (t, 2H), 1.54 (br, 4H), 1.20 (br, 12), 0.82–0.80 (m, 6H). ^{13}C NMR (75 MHz, $CDCl_3$, δ ppm): 164.8, 147.0, 146.8, 144.0, 143.6, 142.5, 137.8, 136.4, 135.6, 129.2, 127.1, 126.2, 125.2, 124.1, 123.1, 122.9, 120.7, 117.5, 115.6, 93.8, 31.9, 30.9, 30.8, 30.0, 29.7, 29.4, 29.1, 25.1, 22.9, 14.4. MS (ESI): m/Z = 672.3. $C_{42}H_{44}N_2O_2S_2$ (M_w = 672.94): calcd. C, 74.96; H, 6.59; N, 4.16; found C, 74.63; H, 6.45; N, 4.62.

*2.2.4.3. (E)-2-Cyano-3-(5′-(4-(diphenylamino)phenyl)-3,4′-dihexyl-2,2′-bithiophene-5-yl)acrylic acid (**DH-43**).* Brown powder. Yield: 78%. ^{1}H NMR (300 MHz, d_6-DMSO, δ ppm): 8.41 (s, 1H), 7.90 (s, 1H), 7.39–7.32 (m, 7H), 7.13–7.07 (m, 6H), 7.02 (d, 2H), 2.81 (t, 2H), 2.68 (t, 2H), 1.59 (m, 4H), 1.28–1.23 (m, 12H), 0.84–0.82 (m, 6H). ^{13}C NMR (75 MHz, $CDCl_3$, δ ppm): 168.9, 147.9, 147.6, 144.6, 142.7, 141.6, 140.5, 139.6, 132.4, 132.1, 131.1, 130.0, 129.7, 127.4, 126.7, 125.2, 123.7, 123.0, 116.1, 96.0, 31.9, 31.2, 30.3, 29.7, 29.6, 29.1, 22.9, 14.4. MS (ESI): m/Z = 673.3. $C_{42}H_{44}N_2O_2S_2$ (M_w = 672.94): calcd. C, 74.96; H, 6.59; N, 4.16; found C, 74.91; H, 6.63; N, 4.14.

*2.2.4.4. (E)-2-Cyano-3-(5′-(4-(diphenylamino)phenyl)-3′,4-dihexyl-2,2′-bithiophene-5-yl)acrylic acid (**DH-44**).* Purple powder. Yield: 70%. ^{1}H NMR (300 MHz, d_6-DMSO, δ ppm): 8.30 (s, 1H), 7.61 (d, 2H), 7.42 (s, 1H), 7.37–7.32 (m, 5H), 7.12–7.06 (m, 6H), 2.81 (t, 4H), 1.61 (br, 4H), 1.28 (br, 12H), 0.85 (m, 6H). ^{13}C NMR (75 MHz, $CDCl_3$, δ ppm): 168.9, 156.8, 148.3, 147.5, 145.2, 145.0, 144.7, 129.6, 129.3, 128.4, 127.3, 127.2, 126.8, 126.3, 125.0, 124.9, 123.7, 123.3, 116.4, 93.9, 31.9, 31.8, 31.5, 30.4, 29.4, 29.2, 22.8, 14.3. MS (ESI): m/Z = 672.3. $C_{42}H_{44}N_2O_2S_2$ (M_w = 672.94): calcd. C, 74.96; H, 6.59; N, 4.16; found C, 74.80; H, 6.77; N, 4.01.

2.3. Fabrication and measurement of DSSCs

Synthesis of the TiO_2 nanoparticles: Typical synthesis of the TiO_2 nanoparticles can be described as follows. A quantity (12.5 mL) of titanium isopropoxide is added at room temperature to 75 mL of a 0.1 M nitric acid solution under vigorous stirring. A white precipitate forms instantaneously. Immediately after the hydrolysis, the slurry is heated to 80 °C and stirred vigorously for 8 h to achieve peptization. Then the slurry was under hydrothermal conditions in an autoclave that was heated for 12 h at 200 °C. The obtained particles were rinsed with water and alcohol, followed by drying at 70 °C.

Preparation of TiO_2 paste for DSSCs: 1.0 g TiO_2 nanoparticles, 0.5 g ethylcellulose, 5 mL ethanol, 3.0 g terpinol and 0.2 mL acetic acid were mixed by ball-milling for 12 h to obtain a homogeneous paste. And the paste for scattering layer was prepared by the same method with replacement of TiO_2 nanoparticles with larger TiO_2 of diameter 200 nm.

Photoelectrode preparation: The preparation of photoelectrode was performed by adopting doctor-blade technique on

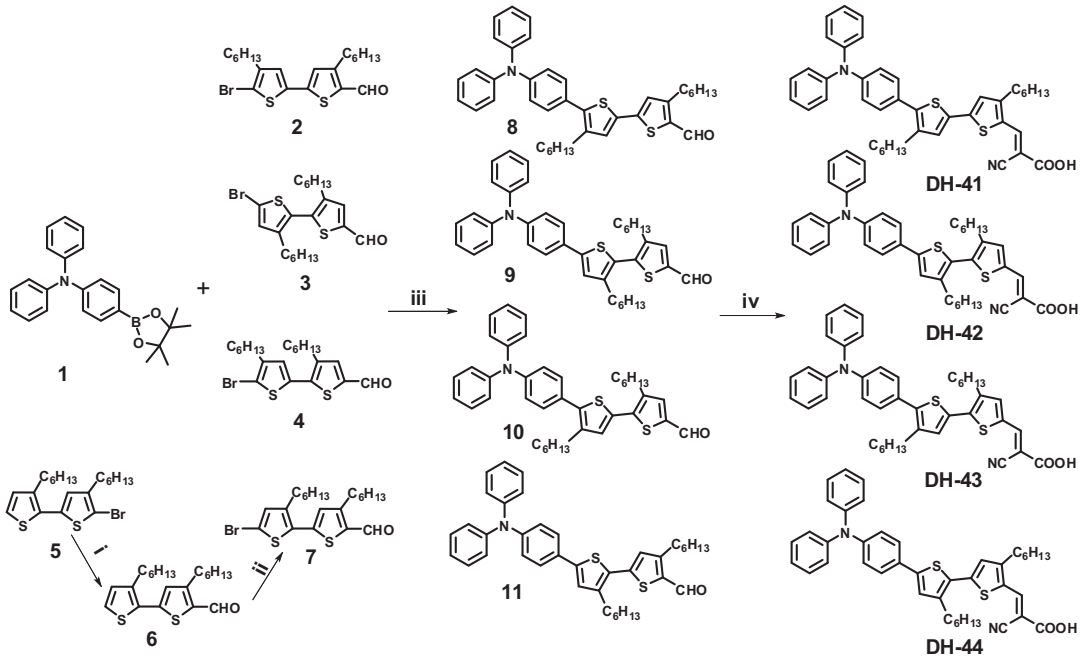

Scheme 1. Synthetic routes for **DH-41**–**DH-42**. Reaction conditions: i) (1) n-BuLi, THF, Ar, −78 °C; (2) DMF; (3) 2 M HCl aqueous solution; ii) NBS, DMF, 0 °C; iii) $Pd(PPh_3)_4$, K_2CO_3 aqueous solution, THF, Ar, 70 °C; iv) cyanoacetic acid, NH_4Ac, HAc, 130 °C.

a conducting glass (FTO, 15–20 Ω $s^{-1}q^{-1}$), which has been rinsed with distilled water and fully soaked in isopropanol for 3 h before using to increase its hydrophilicity. The TiO_2 paste was spread on FTO glass and heated at 500 °C for 30 min, and then a scattering layer was spread on the film and heated at 500 °C for 30 min again. The obtained film was dipped in 50 mM $TiCl_4$ solution at 70 °C for 30 min, followed by calcination at 500 °C for 30 min. Finally the dye-sensitized electrodes were prepared by immersing the obtained films in mixed solution of dyes (ethanol/THF for DH dyes) or N719 (ethanol, 3×10^{-4} mol L^{-1} of all) overnight.

DSSCs fabrication: The dye-sensitized electrode was assembled in a classic sandwich-type cell, that is, the Platinum counter electrode was attached on the dye-sensitized photoanode, after the injection of the electrolyte solution, which consists of 0.5 M LiI, 0.05 M I_2, and 0.1 M 4-tert-butylpyridine in 1:1 acetonitrile-propylene carbonate into the interspace between the photoanode and the counter electrode, the photoelectrochemical property of DSSC was measured.

DSSCs properties test: For the characteristic photocurrent–voltage (*J*–*V*) measurements, the DSSC was illuminated by light with energy of a 100 mW cm^{-2} (AM1.5) from a 300 W solar simulator (Newport, 91160). A computer-controlled Keithley 2400 source meter was employed to collect the *J*–*V* curves. The incident photon-to-current conversion efficiency (IPCE) was measured as a function of wavelength from 320 to 800 nm by using a Model QE/IPCE system (PV Measurements Inc.).

3. Results and discussion

3.1. Synthesis and characterization

Scheme 1 illustrates the synthetic routes of four organic dyes (**DH-41**, **DH-42**, **DH-43** and **DH-44**). The intermediate aldehydes (**2**–**4**) were synthesized according to previous reported

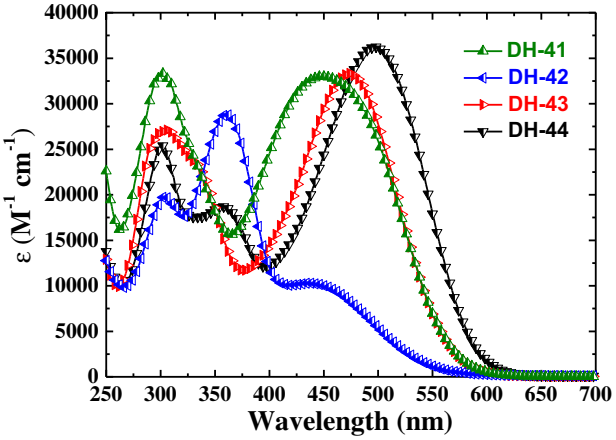

Fig. 2. UV–Vis spectra of DH dyes in solution of DCM.

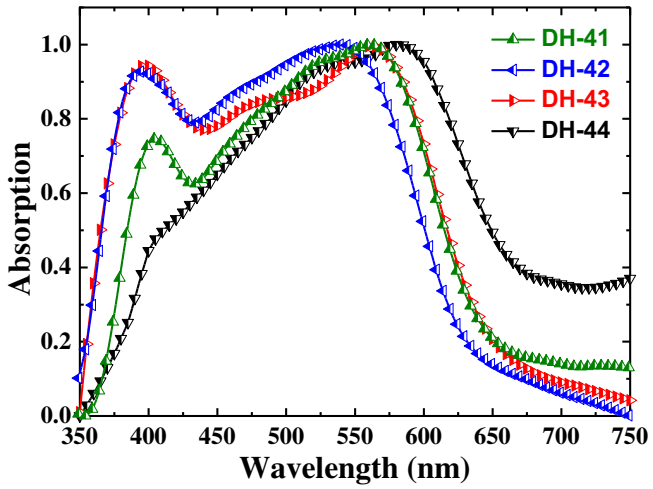

Fig. 3. Normalized absorption profiles of dyes in the TiO_2 film.

Table 1
Optical properties and electrochemical properties of **DH** dyes.

Sample	λ_{max}[a](nm)/ε[b] (10^4 M^{-1} cm^{-1})	λ_{max}[c] (nm)	E_{ox}[d] (V)	E_{opt}[e] (eV)	HOMO[f] (eV)	LUMO[g] (eV)
DH-41	302/3.33, 449/3.30	561	0.82	2.01	−5.25	−3.24
DH-42	360/2.89, 433/1.02	539	0.77	2.12	−5.20	−3.08
DH-43	303/2.71, 475/3.33	565	0.80	2.01	−5.23	−3.22
DH-44	301/2.55, 498/3.62	581	0.78	1.96	−5.21	−3.25

[a] Absorption maxima in solution of DCM.
[b] The molar extinction coefficient at λ_{max} in solution of DCM.
[c] Absorption maxima adsorbed on TiO_2 film.
[d] Oxidation potentials with reference to the ferrocene which was used as an internal standard.
[e] Calculated with the formula $E_{opt} = 1240/\lambda_{onset}$.
[f] Calculated with the formula $E_{HOMO} = -\{E_{ox} + [4.8 - E_{(Fc/Fc+)}]\}$ eV.
[g] Calculated with the formula $E_{LUMO} = (E_{HOMO} + E_{opt})$ eV.

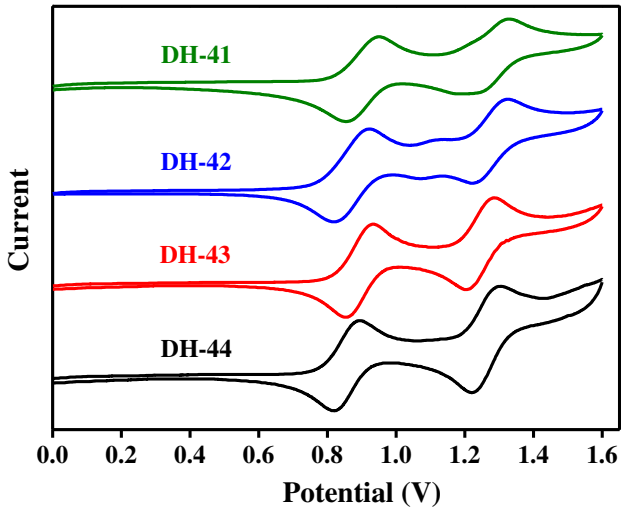

Fig. 4. Cyclic voltammogram of DH dyes.

literatures [25–27]. Another intermediate aldehyde (**7**) was obtained by choosing 5′-bromo-3,4′-dihexyl-2,2′-bithiophene [28] (**5**) as starting material to be converted into **6** and then **7** in two–steps reactions with high yield. The triphenylamine donor was introduced by Suzuki coupling reaction of **2**–**4** or **7** with N,N-diphenyl-4-(4,4,5,5-tetramethyl-1,3,2-dioxaborolan-2-yl)aniline (**1**) to yield the corresponding intermediates of **8**–**10** with high yield. The final organic dyes (**DH-41**, **DH-42**, **DH-43** and **DH-44**) were obtained via Knoevenagel condensation of the corresponding aldehydes (**8**–**10**) with cyanoacetic acid in the presence of ammonium acetate in acetic acid. The structure of all the intermediates and target dyes were confirmed by standard spectroscopic methods and elemental analysis as described in Experimental section.

3.2. Photophysical and electrochemical properties

The UV–Vis absorption spectra of the DH dyes in DCM and absorbed on TiO_2 films are presented in Fig. 2 and Fig. 3, respectively. The absorption maximum and the corresponding molar extinction coefficient data in solution as well as the absorption maximum in thin film for the DH dyes are summarized in Table 1. Each of them exhibited absorption bands at two distinct spectrum regions. One is at about 300–350 nm that can be assigned to the localized aromatic π–π* electron transition of the conjugated molecules. The absorption band above 450 nm is attributed to an intramolecular charge transfer (ICT). As can be seen in Fig. 2, the ICT absorption intensity is greatly weakened for **DH-42** since its molecular coplanarity is destroyed due to the large steric hindrance of two hexyl groups locating at ortho β-positions that makes two thiophene rings of 2,2′-bithiophene unit twisted. However, for some other DH dyes, the molecular coplanarity can be partially maintained because two hexyl groups locate at nonortho β-positions of 2,2′-bithiophene unit. Thus, the ICT absorption intensity is not only strengthened, but is also red shifted. Among them, **DH-44** exhibits the largest ICT intensity and red-shift absorption. The λ_{max} of the DH dyes is in order of **DH-41** < **DH-43** < **DH-44**, indicating that more photons with lower energy can be harvested, which is favorable to improve the performance of DSSCs for the corresponding DH dyes.

After being adsorbed on the surface of TiO_2 film, the maximum absorption coefficient of these stained titania films generally follows the trend of max of dye solutions. Owing to the increased delocalization of the π* orbital of the conjugated framework caused by the interaction between the carboxylate group and the Ti^{4+} ions the energy of the π* level was directly decreased. Therefore, the absorption of all DH sensitizers is dramatically red-shifted as compared with those in solution, and the absorption intensity from 400 to 650 nm is significantly enhanced.

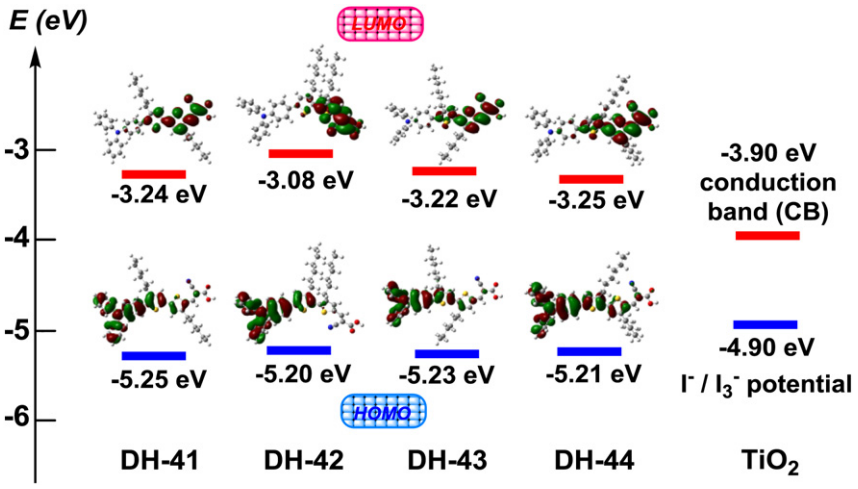

Fig. 5. The energy level diagrams of DH dyes from electrochemical data [29,30].

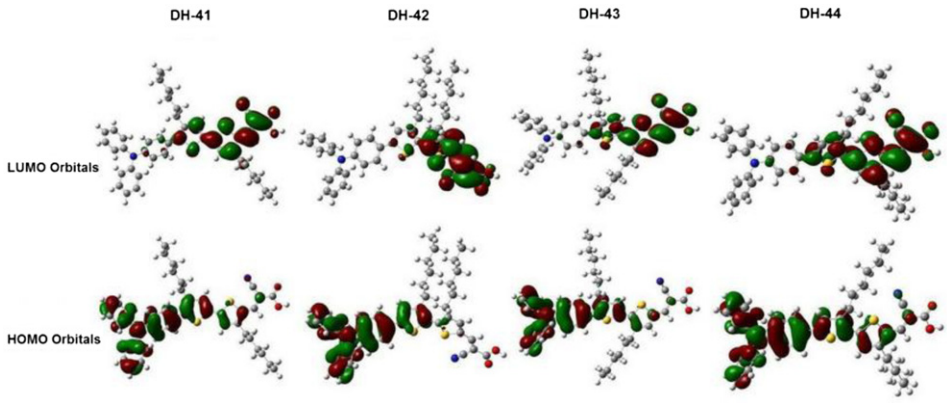

Fig. 6. The frontier orbitals (HOMO and LUMO) of DH dyes.

The redox behavior of DH dyes was studied by cyclic voltammetry (Fig. 4) for the purpose to investigate the ability of electron transfer from the excited dye molecules to the conductive band of TiO_2. The cyclic voltammograms of DH dyes were measured in a solution of 0.1 M n-Bu_4NPF_6 in dichloromethane. A three-electrode cell containing of a Pt-coil working electrode, Pt wire counter electrode and Ag/AgCl reference electrode were employed. The ferrocene/ferricenium (Fc/Fc^+) redox couple was used as an

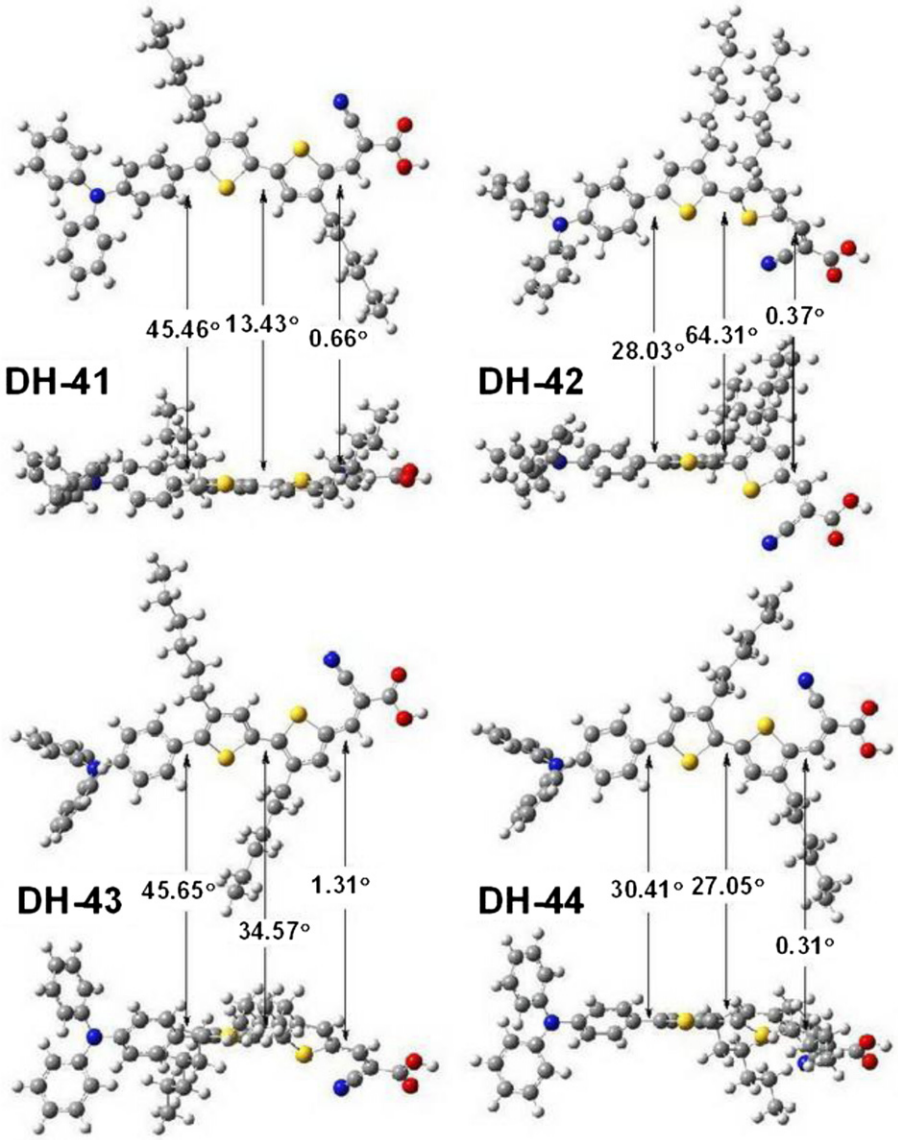

Fig. 7. The optimized structure of DH dyes at the TD-B3LYP/6-31G level.

internal reference. Prior to the electrochemical measurements, all solutions were degassed with high-purity argon.

As can be seen in Fig. 4 and Table 1, the onset oxidative potentials of DH dyes are around 0.80 V that gives the LUMO energies of DH dyes around −3.23 eV, which are higher than the TiO_2 conduction band (−3.9 eV) [29,30] as shown in Fig. 5. This indicates that the electron injection process is energetically favorable compared with the conduction band edge energy level of the TiO_2 electrode (0.5 V vs NHE) [31]. The onset oxidation potential around 0.8 eV can be attributed to the oxidation of the TPA group. And their HOMO energies of around −5.30 eV are lower than I^-/I_3^- potential, suggesting that there is enough driving force for the dye's regeneration.

3.3. Theoretical approaches

The frontier molecular orbitals and optimized structure of DH dyes at the B3LYP/6-31G level are shown in Fig. 6 and Fig. 7, the surfaces are generated with an isovalue of 0.02. As can be seen, the HOMO coefficient is uniformly distributed along the TPA unit at the HOMO state; whereas at the LUMO level, excited electrons are shifted to the π-electron system of the anchoring groups (2,2′-bithiophene-substituted cyanoacrylic acid unit), which is due to the ICT along the π-conjugated skeleton. Therefore, it can be expected that the excited electron will be effectively injected into the conduction band of TiO_2 through the carboxyl anchoring group as well as the adjacent electron-withdrawing cyano group.

Fig. 7 shows the optimized structure of DH dyes. It can be seen that the dihedral angle of two thiophene rings in 2,2′-bithiophene unit is in the order of **DH-41** (13.43°) < **DH-44** (27.05°) < **DH-43** (34.57°) < **DH-42** (64.31°). Among them, two hexyl groups locates at 3,3′-positions of 2,2′-bithiophene unit in **DH-42** exhibits the largest steric hindrance, so its molecular coplanarity is largely destroyed compared with other three DH dyes. Generally, the twisted nonplanar geometric structure can effectively suppress the charge recombination and enhance the open-circuit voltage. In addition, the small dihedral angle of interfacing thiophene with 2-cyanoacrylic acid group for all DH dyes indicates that a hexyl group at different β positions of thiophene group has little influence on the coplanarity of 2-cyanoacrylic acid group with its interfacing thiophene ring. However, the dihedral angle of interfacing thiophene with phenyl ring of TPA group is greatly affected by the hexyl group at different β-position of the thiophene group. For example, **DH-41** and **DH-43** with a hexyl group at 4′-position of

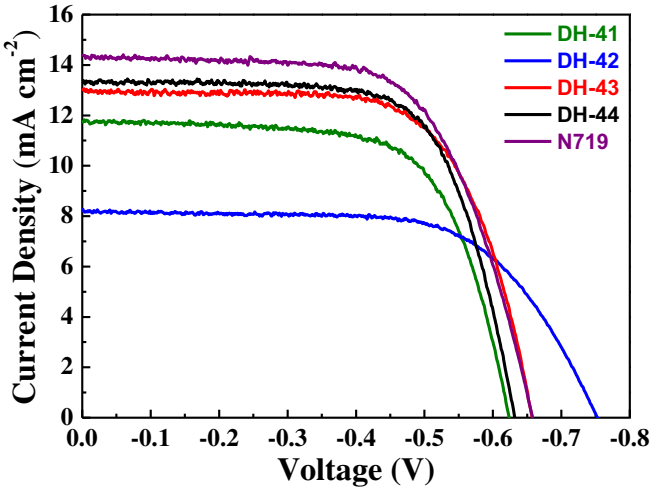

Fig. 8. Photocurrent density–photovoltage curves of DH dyes.

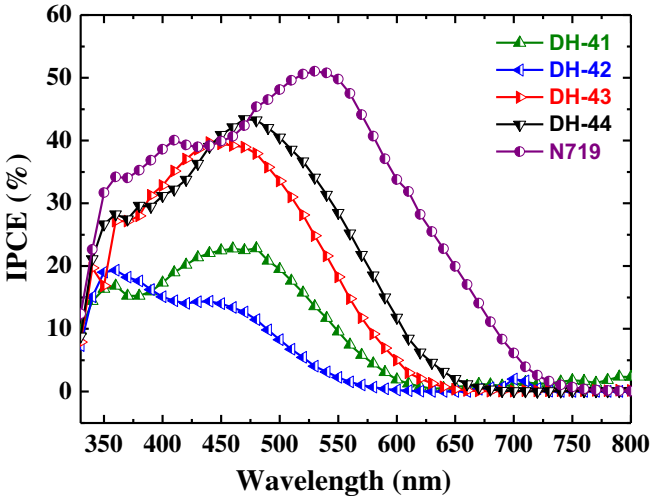

Fig. 9. IPCE spectra of DSSCs based on DH dyes.

2,2′-bithiophene exhibits large steric hindrance with phenyl group, so the dihedral angle of interfacing thiophene with phenyl ring (about 45°) is larger than that (about 30°) of **DH-42** or **DH-44** with a hexyl group at 3′-position of 2,2′-bithiophene. Considering the above three dihedral angles at different segments of the molecular skeleton, it can be concluded that the molecular coplanarity of whole conjugated backbone is most depended on the positions of two hexyl groups in 2,2′-bithiophene unit. Among them, **DH-44** shows the best optimized molecular structure that favors to acquire the largest ICT effect, the most red-shifted absorption and the strongest molar extinction coefficient. This indicates that it will exhibits better photovoltaic performances.

3.4. Photovoltaic performances

The photovoltaic properties of the solar cells were measured under standard AM 1.5G irradiation. The photocurrent density–voltage (J–V) curves and the incident photon to current conversion efficiency (IPCE) spectra of DSSCs based on DH dyes and reference dye **N719** were shown in Fig. 8 and Fig. 9, the detailed photovoltaic parameters are collected in Table 2. As shown in Fig. 8 and Table 2, all the DH dyes show favorable photovoltaic responses and high fill factor (ff) value. Amongst these dyes, **DH-44** exhibits an impressive photovoltaic performance with a short circuit current density (J_{sc}) of 13.38 mA cm^{-2}, an open circuit voltage (V_{oc}) of 0.63 V and a fill factor (ff) of 0.64, resulting in an overall power conversion efficiency (η) of 5.86% (above 95% of the standard device from **N719**, 6.15%). Also, both **DH-41** (J_{sc} = 11.77 mA cm^{-2}, V_{oc} = 0.62 V, η = 4.96%) and **DH-43** (J_{sc} = 12.96 mA cm^{-2}, V_{oc} = 0.63 V, η = 5.78%) shows good performance. The high short circuit current density (J_{sc}) for **DH-41**, **DH-43** and **DH-44** can be mainly attributed to its coplanar structure that causes more efficient light-harvesting, stronger ICT absorption and higher molar extinction co-efficiency. Only **DH-42** based cell shows relatively

Table 2
Photovoltaic performances of DSSCs based on DH dyes and N719.

Sample	J_{sc} (mA cm^{-2})	V_{oc} (V)	FF	Efficiency (%)
DH-41	11.77	0.62	0.68	4.96
DH-42	8.22	0.75	0.65	4.00
DH-43	12.96	0.66	0.68	5.78
DH-44	13.38	0.63	0.70	5.86
N719	14.35	0.66	0.65	6.15

poor photovoltaic performances (J_{sc} = 8.22 mA cm^{-2}, V_{oc} = 0.75 V, η = 4.00%), since the introduction of two substituted long-chain alkyl groups at ortho β-positions of 2,2′-bithiophene unit in **DH-42** almost completely destroys the coplanarity of conjugated skeleton that is unfavorable for broadening its UV–Vis absorption with high extinction coefficient. However, the twisted nonplanar structure can result in the charge separation of the dye molecule and suppress the charge recombination. This is beneficial to the enhancement of an open circuit voltage (V_{oc}) [16,32]. Thus, the V_{oc} of 0.75 V for **DH-42** is much higher than that of the other three DH dyes (V_{oc} = 0.62–0.66 V) [33]. It should be noteworthy that these photovoltaic performances for DH dyes are well in agreement with the above results of theoretical calculation, indicating that the optimization of the dye's molecular structure via changing the substituted position of alkyl group at 2,2′-bithiophene linker can effectively improve the DSSCs performances.

4. Conclusions

In this work we employ TPA group as an electron-donor, cyanoacrylic acid unit as an electron-acceptor and β-substituted 2,2′-bithiophene unit as a π-linker, respectively, to construct a series of metal-free organic dyes (**DH-41**, **DH-42**, **DH-43** and **DH-44**). Changing β-substituted position of hexyl group at 2,2′-bithiophene linker not only alters the molecular coplanarity of the dyes, but it also adjusts the ICT effect and absorption property, and finally modifies the photovoltaic performance. Amongst the DH dyes, **DH-44** shows the best optimized structure for DSSCs and produces high power conversion efficiency of 5.86%, which reaches over 95% of the reference dye N719-based cell fabricated and measured under the same conditions. This work demonstrates that 2,2′-bithiophene group is a good π-linker for organic dyes and the optimization of molecular structure via changing β-substituted position of alkyl group is an effective approach to improve the DSSCs performances.

Acknowledgments

We are grateful to the National Natural Science Foundation of China (Nos. 20972122 and 51173138), and the Specialized Research Fund for the Doctoral Program of Higher Education of China (No. 20100141110010) for financial support.

References

[1] B.O. Regan, M. Grätzel, Nature 353 (1991) 737–740.
[2] L. Moreira Gonçalves, V. de Zea Bermudez, H. Aguilar Ribeiro, A. Magalhães Mendes, Energy Environ. Sci. 1 (2008) 655–667.
[3] M.K. Nazeeruddin, C. Klein, P. Liska, M. Grätzel, Coord. Chem. Rev. 249 (2005) 1460–1467.
[4] N. Robertson, Angew. Chem. Int. Ed. 45 (2006) 2338–2345.
[5] Y. Ooyama, Y. Harima, Eur. J. Org. Chem. 18 (2009) 2891–2897.
[6] T. Horiuchi, H. Miura, S. Uchida, Chem. Commun. (2003) 3036–3037.
[7] S. Ito, H. Miura, S. Uchida, M. Tanaka, K. Sumioka, P. Liska, P. Comte, P. Péchy, M. Grätzel, Chem. Commun. (2008) 5194–5196.
[8] A. Mishra, M.K.R. Fischer, P. Bäuerle, Angew. Chem. Int. Ed. 48 (2009) 2474–2499.
[9] H. Qin, S. Wenger, M. Xu, F. Gao, X. Jing, P. Wang, S.M. Zakeeruddin, M. Grätzel, J. Am. Chem. Soc. 130 (2008) 9202–9203.
[10] J.H. Yum, D.P. Hagberg, S.J. Moon, K.M. Karlsson, T. Marinado, L.C. Sun, A. Hagfeldt, M.K. Nazeeruddin, M. Grätzel, Angew. Chem. Int. Ed. 48 (2009) 1576–1580.
[11] G.L. Zhang, H. Bala, Y.M. Cheng, D. Shi, X.J. Lv, Q.J. Yu, P. Wang, Chem. Commun. 16 (2009) 2198–2200.
[12] H. Im, S. Kim, C. Park, S.H. Jang, C. J.Kim, K. Kim, N.G. Park, C. Kim, Chem. Commun. 46 (2010) 1335–1337.
[13] W.D. Zeng, Y.M. Cao, Y. Bai, Y.H. Wang, Y.S. Shi, M. Zhang, F.F. Wang, C. Y.Pan, P. Wang, Chem. Mater. 22 (2010) 1915–1925.
[14] T. Daeneke, T.H. Kwon, A.B. Holmes, N.W. Duffy, U. Bach, L. Spiccia, Nat. Chem. 3 (2011) 211–215.
[15] D. Heredia, J. Natera, M. Gervaldo, L. Otero, F. Fungo, C.Y. Lin, K.T. Wong, Org. Lett. 12 (2010) 12–15.
[16] M. Velusamy, K.R.J. Thomas, J.T. Lin, Y.C. Hsu, K.C. Ho, Org. Lett. 7 (2005) 1899–1902.
[17] T. Duan, K. Fan, Y. Fu, C. Zhong, X. Chen, T. Peng, J. Qin, Dyes Pigm. 94 (2012) 28–33.
[18] M.F. Xu, R.Z. Li, N. Pootrakulchote, D. Shi, J. Guo, Z.H. Yi, S.M. Zakeeruddin, M. Grätzel, P. Wang, J. Phys. Chem. C 112 (2008) 19770–19776.
[19] E. Kozma, I. Concina, A. Braga, L. Borgese, L.E. Depero, A. Vomiero, G. Sberveglieri, M. Catellani, J. Mater. Chem. 21 (2011) 13785–13788.
[20] J. Nishida, T. Masuko, Y. Cui, K. Hara, H. Shibuya, M. Ihara, T. Hosoyama, R. Goto, S. Mori, Y. Yamashita, J. Phys. Chem. C 114 (2010) 17920–17925.
[21] Z.S. Wang, N. Koumura, Y. Cui, M. Takahashi, H. Sekiguchi, A. Mori, T. Kubo, A. Furube, K. Hara, Chem. Mater. 20 (2008) 3993–4003.
[22] X.H. Zhang, Z.S. Wang, Y. Cui, N. Koumura, A. Furube, K. Hara, J. Phys. Chem. C 113 (2009) 13409–13415.
[23] X.Y. Jing, J.Y. Liu, D.F. Zhou, F.F. Wang, F. Fabregat-Santiago, S.G. Miralles, J. Bisquert, P. Wang, J. Phys. Chem. C 115 (2011) 14425–14430.
[24] J. Lee, J. Kim, G. Kim, C. Yang, Tetrahedron 66 (2010) 9440–9444.
[25] N. Hayashi, T. Nishihara, T. Matsukihira, H. Nakashima, K. Miyabayashi, M. Miyake, H. Higuchi, Bull. Chem. Soc. Jpn. 80 (2007) 371–386.
[26] J. Zhang, D. Deng, C. He, Y.J. He, M.J. Zhang, Z.G. Zhang, Z.J. Zhang, Y.F. Li, Chem. Mater. 23 (2011) 817–822.
[27] J.J. Ko, D.H. Kim, H.B. Choi, Repub. Korean Kongkae Taeho Kongbo (2010). KR20100127474.
[28] O. Hagemann, M. Jorgensen, F.C. Krebs, J. Org. Chem. 71 (2006) 5546–5559.
[29] F. Lenzmann, J. Krueger, S. Burnside, K. Brooks, M. Grätzel, D. Gal, S. Ruhle, D. Cahen, J. Phys. Chem. B 105 (2001) 6347–6352.
[30] D. Kumaresan, R.P. Thummel, T. Bura, G. Ulrich, R. Ziessel, Chem.-Eur. J. 15 (2009) 6335–6339.
[31] Z.S. Wang, Y. Cui, Y. Dan-Oh, C. Kasada, A. Shinpo, K. Hara, J. Phys. Chem. C 112 (2008) 17011–17017.
[32] H. Ozeki, A. Nomoto, K. Ogawa, Y. Kobuke, M. Murakami, K. Hosoda, M. Ohtani, S. Nakashima, H. Miyasaka, T. Okada, Chem. -Eur. J. 10 (2004) 6393–6401.
[33] M. Xu, M. Zhang, M. Pastore, R. Li, F. De Angelis, P. Wang, Chem. Sci. 3 (2012) 976–983.